8. Haas D, Hoffmann GF (2006) Mevalonate kinase deficiencies: from mevalonic aciduria to hyperimmunoglobulinemia D syndrome. Orphanet J Rare Dis 1:13
9. Cuisset L, Drenth JP, Simon A, Vincent MF, Van der Velde Visser S, Van der Meer JW (2001) Molecular analysis of MVK mutations and enzymatic activity in hyper-IgD and periodic fever syndrome. Eur J Hum Genet 9(4):260–266
10. Drenth JP, Cuisset L, Grateau G, Vasseur C, van de Velde-Visser SD, de Jong JG et al (1999) Mutations in the gene encoding mevalonate kinase cause hyper-IgD and periodic fever syndrome. International Hyper-IgD Study Group. Nat Genet 22:178–181
11. Takada K, Aksentijevich I, Mahadevan V, Dean JA, Kelley RI, Kastner DL (2003) Favorable preliminary experience with etanercept in two patients with the hyperimmunoglobulinemia D and periodic fever syndrome. Arthritis Rheum 48:2645–2651
12. Drenth JP, Haagsma CJ, van der Meer JW (1994) Hyperimmunoglobulinemia D and periodic fever syndrome. The clinical spectrum in a series of 50 patients. International Hyper-IgD Study Group. Medicine (Bartimore) 73:133–144
13. Naruto T, Nakagishi Y, Mori M, Miyamae T, Imagawa T, Yokota S (2009) Hyper-IgD syndrome with novel mutation in Japanese girl. Mod Rheumatol 19(1):96–99

Mod Rheumatol (2011) 21:641–645
DOI 10.1007/s10165-011-0442-7

CASE REPORT

Patient with neonatal-onset chronic hepatitis presenting with mevalonate kinase deficiency with a novel MVK gene mutation

Masahiro Tahara · Hidemasa Sakai · Ryuta Nishikomori · Takahiro Yasumi · Toshio Heike · Ikuo Nagata · Ayano Inui · Tomoo Fujisawa · Yosuke Shigematsu · Koji Nishijima · Katsuji Kuwakado · Shinichi Watabe · Junji Kameyama

Received: 24 November 2010 / Accepted: 22 February 2011 / Published online: 12 March 2011

Abstract A Japanese girl with neonatal-onset chronic hepatitis and systemic inflammation was diagnosed with hyper-immunoglobulinemia D and periodic fever syndrome (HIDS). However, she lacked the typical HIDS features until the age of 32 months. She had compound heterozygous MVK mutations, H380R and A262P, the latter of which was novel. These findings suggest that HIDS patients could lack typical episodes of recurrent fever at the onset and that HIDS should be considered as a possible cause of neonatal-onset chronic hepatitis.

M. Tahara · K. Nishijima · K. Kuwakado · S. Watabe · J. Kameyama
Department of Pediatrics, Kurashiki Central Hospital, Kurashiki, Japan

M. Tahara (✉)
Department of Pediatrics, Tsuchiya General Hospital, 3-30 Nakashima, Naka-ku, Hiroshima 730-8655, Japan
e-mail: mttahara@qg7.so-net.ne.jp

H. Sakai · R. Nishikomori · T. Yasumi · T. Heike
Department of Pediatrics, Kyoto University Graduate School of Medicine, Kyoto, Japan

I. Nagata
Division of Pediatrics and Perinatology, Faculty of Medicine, Tottori University, Yonago, Japan

A. Inui · T. Fujisawa
Department of Pediatrics, Yokohama City Tobu Hospital, Yokohama, Japan

Y. Shigematsu
Department of Health Science, Faculty of Medicine Sciences, University of Fukui, Fukui, Japan

Keywords Autoimmune hepatitis · Hyper-IgD syndrome · Liver biopsy · MVK gene · Neonatal-onset chronic hepatitis

Abbreviations

HIDS	Hyper-immunoglobulinemia D and periodic fever syndrome
IgD	Immunoglobulin D
MVK	Mevalonate kinase
FMF	Familial Mediterranean fever
MEFV	Familial Mediterranean fever gene
AIH	Autoimmune hepatitis
CRP	C-reactive protein

Introduction

Mevalonate kinase deficiency is an autosomal recessive metabolic disorder caused by mevalonate kinase (MVK) gene mutations. The disorder presents as a phenotypic spectrum in which mevalonic aciduria is the more severe form, with neurological complications, and hyperimmunoglobulinemia D and periodic fever syndrome (HIDS) is the milder form. HIDS is characterized by recurrent febrile attacks, with lymphadenopathy, abdominal symptoms, skin eruptions, and joint involvement [1]. In this report, we describe a patient with a severe form of HIDS caused by a novel MVK mutation; the patient had presented with neonatal-onset chronic hepatitis that was temporarily diagnosed as autoimmune hepatitis (AIH). The lack of typical recurrent fever and rashes at the onset of the disease delayed the diagnosis of HIDS, which alerted the clinicians that HIDS could exist in patients with continuous inflammatory episodes even with atypical clinical courses.

Case report

A Japanese girl was born at 36 weeks' gestation with a weight of 2,240 g. Her parents were non-consanguineous and the family history was unremarkable. At birth she had no symptoms, but physical examination revealed hepatomegaly (1.5 cm below the right costal margin) without splenomegaly. No jaundice, ascites, or coagulation abnormalities were present. Laboratory examinations showed increased white blood cell count (45,700/mm^3) and serum C-reactive protein (CRP) (15.8 mg/dl), as well as increased transaminase levels (aspartate aminotransferase [AST] 207 IU/l, alanine aminotransferase [ALT] 96 IU/l), lactate dehydrogenase (LDH) (6,575 IU/l), and biliary enzyme levels (γ-guanosine triphosphate [GTP] 61 IU/l). An increased immunoglobulin M level (53.0 mg/dl) caused us to work on congenital infections, with bacterial cultures of blood, cerebrospinal fluid (CSF), and gastric fluid, and determination of serum β D-glucan, and measurements of serum antibodies against cytomegalovirus, toxoplasmosis, syphilis, rubella, herpes simplex type I and type II, listeriosis, Epstein-Barr virus, adenovirus, hepatitis A and B and C viruses, *Chlamydia trachomatis*, and mycoplasma, all of which were negative. Radiographic work-up with computed tomography (CT), magnetic resonance imaging (MRI), and gallium scintigraphy, as well as bone-marrow aspirate examination, did not reveal any congenital neoplasm. A search for metabolic disorders by measurements of blood amino acids and urinary organic acids was negative.

Without any specific treatments, the hepatomegaly gradually increased, although abdominal MRI revealed diffuse inflammation of the liver. To explore further the cause of the hepatomegaly, a needle liver biopsy was performed at the age of 6 months. The biopsied liver specimen showed the presence of mild lymphocytic infiltration and fibrosing lesions in the portal area, and short septa extending from a slightly enlarged portal tract (Fig. 1a, b), which indicated a diagnosis of chronic hepatitis without specific causes.

At the age of 14 months, splenomegaly appeared, and elevated serum IgG (2,299 mg/dl) as well as anti-smooth muscle antibodies (1:160) were detected, which led us to diagnose the patient as having AIH [2]. The patient received methylprednisolone pulse therapy, followed by prednisolone and azathioprine for the presumed AIH [3]. Serum transaminase levels normalized in response to the treatment, although cervical lymphadenopathy, hepatosplenomegaly, and elevated serum CRP persisted.

The continuous elevation of CRP prompted us to consider autoinflammatory diseases; thus, we performed genetic analysis for familial Mediterranean fever (FMF), tumor necrosis factor (TNF) receptor-associated periodic syndrome, and cryopyrin-associated periodic syndrome, at the age of 26 months. After obtaining written informed consent from the parents and approval from the Institutional Review Board of Kyoto University, peripheral blood samples were collected from the patient and her parents for genetic analysis. The analysis was done by sequencing all the exons, including exon–intron junctions, which showed heterozygous L110P and E148Q missense mutations on the familial Mediterranean fever (MEFV) gene (Fig. 2a) without any mutations of the TNFRSF1A and NLRP3

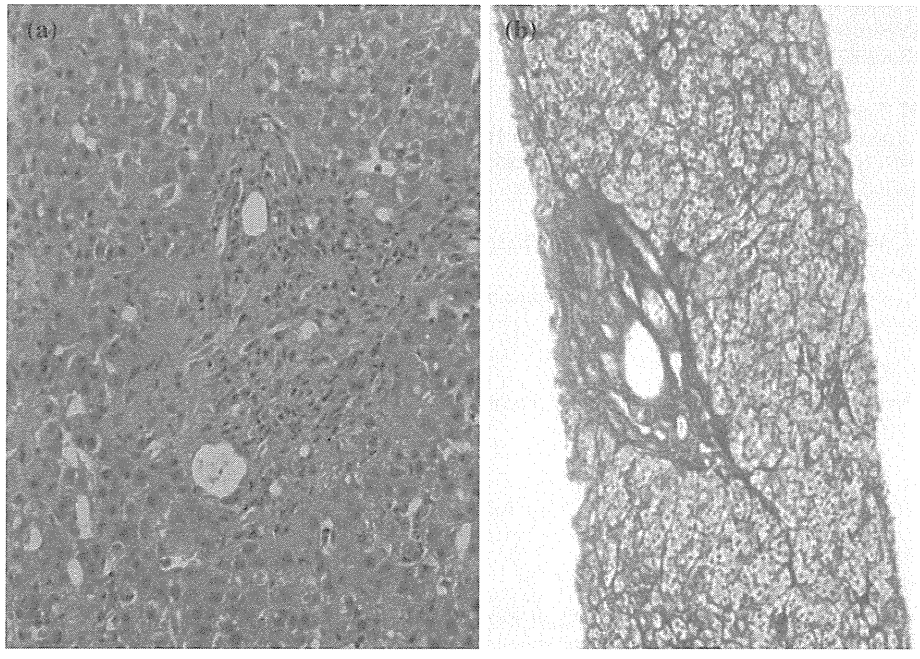

Fig. 1 Liver biopsy specimen showing chronic hepatitis. **a** The portal tract is infiltrated with lymphocytes (H&E, ×200). **b** Short septa extend from the slightly enlarged portal tract (reticulum, ×100)

genes. The L110P and E148Q mutations on MEFV were considered to be single-nucleotide polymorphisms (SNPs), based upon the prevalence of the mutations, as well as their weak association with FMF in Japan. Because none of periodic fever, rashes, gastrointestinal symptoms, or elevated serum IgD was observed at that time, the MVK gene was not examined.

The patient continued to show a good response to the AIH treatments, although tapering off the prednisone induced periodic fever with maculopapular rashes approximately once a month, shown for the first time at the age of 32 months. The fever episodes persisted for 3–5 days and the duration of the fever was reduced to 1–2 days by temporarily increasing the dose of prednisone. Serum CRP levels were around 20 mg/dl at the onset of fever, and 1–4 mg/dl in the asymptomatic period. The newly emerged clinical symptoms and the good response to the systemic steroid prompted us to consider HIDS. Full examination for HIDS showed: (1) elevated serum IgD (19.2 mg/dl) (control 0–9 mg/dl); (2) increased urinary mevalonic acid (49.1 μg/mg creatinine) (control 0.091 ± 0.028 μg/mg creatinine); and (3) a significant decrease in the mevalonate kinase activity of peripheral blood mononuclear cells (PBMCs; below the detection limit). Genetic analysis of the MVK gene revealed compound heterozygous mutations, A262P and H380R, the former of which was a novel mutation (Fig. 2b). The MVK mutations were not identified in 100 healthy Japanese controls. Finally we diagnosed the patient with HIDS, at the age of 6 years. We treated the patient with simvastatin (0.07 mg/kg/day), which was partially effective in reducing the frequency of the periodic fever. Although no decline in urinary mevalonic acid has been produced by simvastatin (33.7–107.8 μg/mg creatinine), the patient has had a benign course, without mental retardation or neurological impairments (Fig. 3).

To see if the patient's liver abnormalities were due to either AIH or HIDS, we performed an immunohistological analysis of the biopsied liver specimen. It was stained for CD68, and unstained for CD3 and CD79 (Fig. 4). These

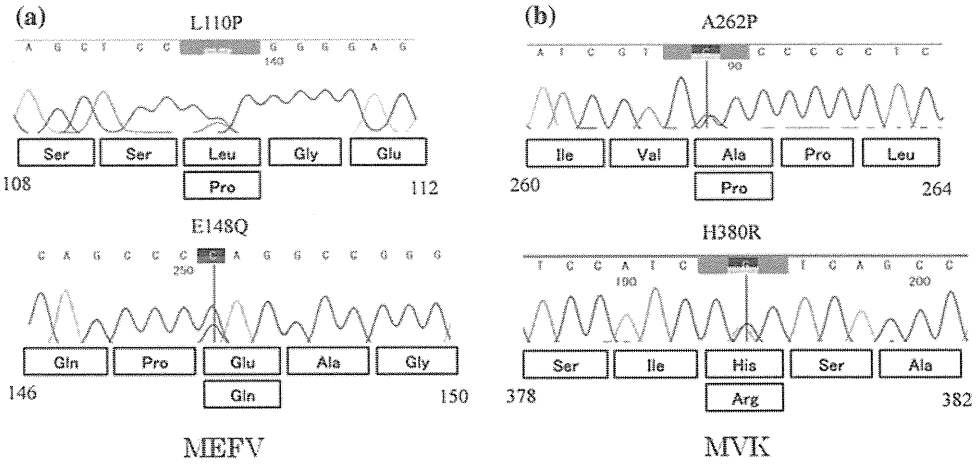

Fig. 2 Genetic analysis. **a** Genetic analysis of the MEFV gene. The patient had heterozygous amino acid changes of L110P and E148Q. **b** Genetic analysis of the MVK gene. The patient had heterozygous mutations of A262P and H380R

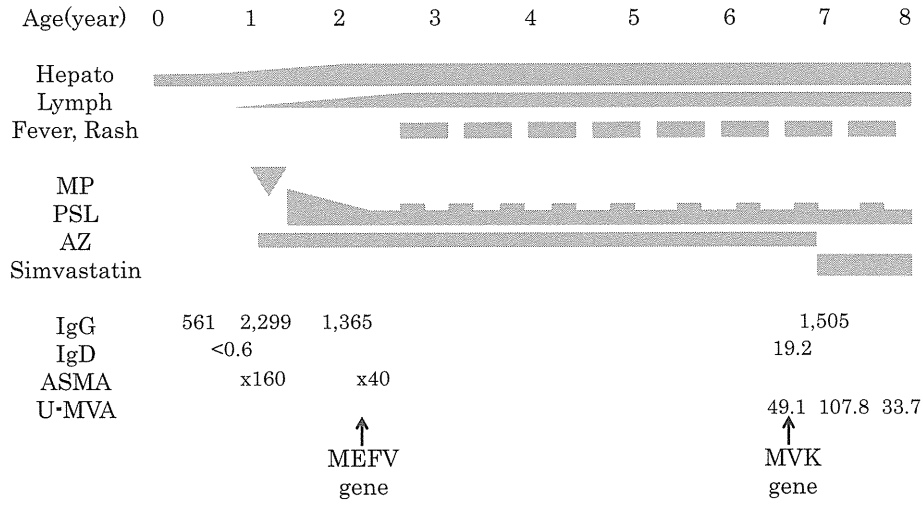

Fig. 3 Clinical course. *Hepato* Hepatosplenomegaly, *Lymph* cervical lymphadenopathy, *MP* methylprednisolone, *PSL* prednisolone, *AZ* azathioprine, *ASMA* anti-smooth muscle antibody, *U-MVA* urinary mevalonic acid (μg/mg creatinine)

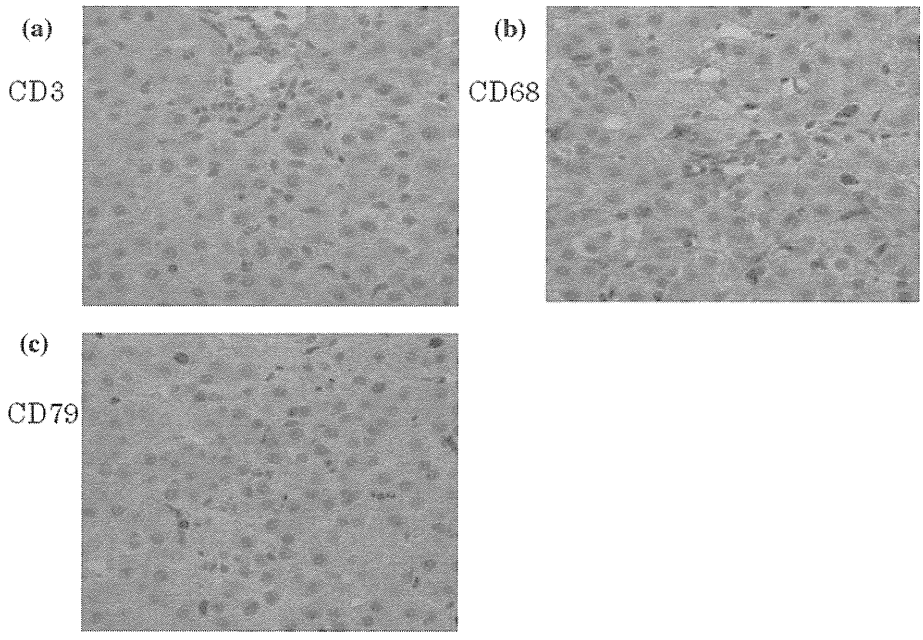

Fig. 4 Immunohistochemical analysis of the biopsied liver tissues. **a** CD3 (×400), **b** CD68 (×400), **c** CD79 (×400)

data led us to conclude that the hepatitis seemed to be a manifestation of HIDS, rather than resulting from an autoimmune response.

Discussion

We have reported here a Japanese girl who was diagnosed with HIDS by genetic analysis, as well as by laboratory examinations such as mevalonate kinase activity and urinary excretion of mevalonate. According to the report of the Japanese HIDS registry, the 4 most prevalent MVK mutations (V377I, I268T, H20P/N, and P167L) accounted for 71.5% of the mutations found. Our patient had a very rare genotype among the patients on the HIDS registry, as the H380R mutation was identified in 1.5% of the patients and A262P was a novel mutation. Because mevalonate kinase activity was below the detection limit, mevalonic aciduria could have been considered as the diagnosis in our patient. However, the mevalonic acid level in the urine was not as high as that reported for patients with mevalonic aciduria [4] and the clinical features of our patient lacked the neurological and developmental abnormalities that are distinctive signs of mevalonic aciduria. Thus, we concluded that the patient suffered from a severe form of HIDS, although we note that mevalonate kinase deficiency presents as a phenotypic continuum in which disease severity ranges from mevalonic aciduria to HIDS [5].

Serum transaminase levels in our patient were elevated since birth, which is relatively rare for HIDS, and liver biopsy showed chronic non-specific hepatitis [6]. Although the serum transaminase levels were improved by the treatment for AIH, the histological and immunohistochemical findings were not typical of AIH [6], which is a generally unresolving inflammation of the liver of unknown cause [7]. There have been some reports of HIDS patients with liver abnormalities. Topaloglu et al. [8] reported a similar case of HIDS in a patient who had neonatal hepatosplenomegaly without fever at the beginning, and they performed liver biopsy which showed portal fibrosis. Hinson et al. [9] reported two patients with mevalonate kinase deficiency who had neonatal hepatosplenomegaly and elevated transaminase levels; liver biopsy showed chronic active cholestatic hepatitis and portal fibrosis, respectively.

Neonatal hepatitis is a syndrome associated with a history that includes any type of infectious, genetic, toxic, or metabolic causation. Neonatal hepatitis is characterized by clinical and laboratory findings of liver dysfunction, particularly conjugated hyperbilirubinemia. In our patient, the clinical course in early childhood was not typical of neonatal hepatitis. But the clinical course in our patient suggests that it is important to include HIDS in the differential diagnosis of neonatal hepatitis or neonatal-onset chronic hepatitis.

Genetic analysis of autoinflammatory disease genes in our patient revealed 2 heterozygous amino acid changes, L110P and E148Q, in the MEFV gene, which were shared with the patient's asymptomatic mother. It has been reported that the allele frequency of E148Q in the Japanese population was high (16.38%), and both E148Q and L110P are considered as SNPs [10]. On the other hand, Touitou et al. [11] demonstrated that E148Q may have an exacerbating effect on FMF when it is part of complex alleles. In addition, there are other reports that mutations in 2 autoinflammatory

genes cause more severe diseases [8, 12]. Thus, the heterozygous E148Q and L110P amino acid changes in the MEFV gene may cause a more severe form of HIDS.

The name 'HIDS' was given to the disorder because of the observed elevation in serum IgD, before the identification of the disease-causing mutations in the MVK gene. In a study of 103 HIDS patients, 22% had normal serum IgD, particularly during infancy [13], which indicates that serum IgD is not sensitive enough for diagnosing HIDS. In Asian countries like Japan, HIDS is so rare that clinicians do not know the clinical relevance of IgD in relation to the diagnosis of HIDS. Therefore, it is very important to let clinicians know that more specific and more sensitive diagnostic tests; namely, measurement of urinary mevalonic acid and/or genetic analysis of the MVK gene are necessary to diagnose HIDS. It should also be pointed out that both the measurements of urinary mevalonic acid and the genetic tests of the MVK gene require special laboratory equipment, which makes it difficult to access such diagnostic tests.

In conclusion, we have reported a patient with a severe form of HIDS who presented with neonatal-onset chronic hepatitis with a novel MVK mutation. HIDS should be included in the differential diagnosis of neonatal-onset chronic hepatitis, even if the serum IgD is within the normal range and typical recurrent fever is not identified.

Acknowledgments We are grateful to Dr. Hans R. Waterham for measurement of mevalonate kinase activity.

Conflict of interest The authors have no conflicts of interest to declare.

References

1. Drenth JP, Denecker NE, Prieur AM, van der Meer JW. Hyperimmunoglobulin D syndrome. Presse Med. 1995;24:1211–3.
2. Alvarez F, Berg PA, Bianchi FB, Bianchi L, Burroughs AK, Cancado EL, et al. International Autoimmune Hepatitis Group report: review of criteria for diagnosis of autoimmune hepatitis. J Hepatol. 1999;31:929–38.
3. Sogo T, Fujisawa T, Inui A, Komatsu H, Etani Y, Tajiri H, et al. Intravenous methylprednisolone pulse therapy for children with autoimmune hepatitis. Hepatol Res. 2006;34:187–92.
4. Houten SM, Wanders RJA, Waterham HR. Biochemical and genetic aspects of mevalonate kinase and its deficiency. Biochim Biophys Acta. 2000;1529:19–32.
5. Simon A, Kremer HPH, Wevers RA, Scheffer H, de Jong JG, van der Meer JWM, et al. Mevalonate kinase deficiency: evidence for a phenotypic continuum. Neurology. 2004;62:994–7.
6. Kage M. Pathology of autoimmune liver diseases in children. Hepatol Res. 2007;37:S502–8.
7. Manns MP, Czaja AJ, Gorham JD, Krawitt EI, Mieli-Vergani G, Vergani D, et al. Diagnosis and management of autoimmune hepatitis. Hepatology. 2010;51:2193–213.
8. Topaloglu R, Ayaz NA, Waterham HR, Yuce A, Gumruk F, Sanal O. Hyperimmunoglobulinemia D and periodic fever syndrome; treatment with etanercept and follow-up. Clin Rheumatol. 2008;27:1317–20.
9. Hinson DD, Rogers ZR, Hoffmann GF, Schachtele M, Fingerhut R, Kohlschtter A, et al. Hematological abnormalities and cholestatic liver disease in two patients with mevalonate kinase deficiency. Am J Med Genet. 1998;78:408–12.
10. Komatsu M, Takahashi T, Uemura N, Takada G. Familial Mediterranean fever medicated with an herbal medicine in Japan. Pediatr Int. 2004;46:81–4.
11. Touitou I. The spectrum of familial Mediterranean fever (FMF) mutations. Eur J Hum Genet. 2001;9:473–83.
12. Stojanov S, Lohse P, Lohse P, Hoffmann F, Renner ED, Zellerer S, et al. Molecular analysis of the MVK and TNFRSF1A genes in patients with a clinical presentation typical of the hyperimmunoglobulinemia D with periodic fever syndrome: a low-penetrance TNFRSF1A variant in a heterozygous MVK carrier possibly influences the phenotype of hyperimmunoglobulinemia D with periodic fever syndrome or vice versa. Arthritis Rheum. 2004;50:1951–8.
13. Van der Hilst JC, Bodar EJ, Barron KS, Frenkel J, Drenth JP, van der Meer JW, International HIDS Study Group, et al. Long-term follow-up, clinical features, and quality of life in a series of 103 patients with hyperimmunoglobulinemia D syndrome. Medicine (Baltimore). 2008;87:301–10.

J Clin Immunol (2011) 31:762–772
DOI 10.1007/s10875-011-9560-4

Decreased Expression in Nuclear Factor-κB Essential Modulator Due to a Novel Splice-Site Mutation Causes X-linked Ectodermal Dysplasia with Immunodeficiency

Shuhei Karakawa · Satoshi Okada · Miyuki Tsumura · Yoko Mizoguchi · Norioki Ohno · Shin'ichiro Yasunaga · Motoaki Ohtsubo · Tomoki Kawai · Ryuta Nishikomori · Takemasa Sakaguchi · Yoshihiro Takihara · Masao Kobayashi

Received: 6 March 2011 / Accepted: 14 June 2011 / Published online: 1 July 2011

Abstract X-linked ectodermal dysplasia with immunodeficiency (XL-ED-ID) is caused by hypomorphic mutations in *NEMO*, which encodes nuclear factor-kappaB (NF-κB) essential modulator. We identified a novel mutation, 769−1 G>C, at the splicing acceptor site of exon 7 in *NEMO* in a Japanese patient with XL-ED-ID. Although various abnormally spliced NEMO messenger RNAs (mRNAs) were observed, a small amount of wild-type (WT) mRNA was also identified. Decreased NEMO protein expression was detected in various lineages of leukocytes. Although one abnormally spliced NEMO protein showed residual NF-κB transcription activity, it did not seem to exert a dominant-negative effect against WT-NEMO activity. $CD4^+$ T cell proliferation was impaired in response to measles and mumps, but not rubella. These results were consistent with the clinical and laboratory findings of the patient, suggesting the functional importance of NEMO against specific viral infections. The 769−1 G>C mutation is responsible for decreased WT-NEMO protein expression, resulting in the development of XL-ED-ID.

Keywords NEMO · XL-ED-ID · *IKBKG* · splice-site mutation · measles

Electronic supplementary material The online version of this article (doi:10.1007/s10875-011-9560-4) contains supplementary material, which is available to authorized users.

S. Karakawa · S. Okada (✉) · M. Tsumura · Y. Mizoguchi · N. Ohno · M. Kobayashi
Department of Pediatrics,
Hiroshima University Graduate School of Biomedical Sciences,
1-2-3 Kasumi, Minami-ku,
Hiroshima 734-8551, Japan
e-mail: s-okada@pg8.so-net.ne.jp

S. Yasunaga · M. Ohtsubo · Y. Takihara
Department of Stem Cell Biology, Research Institute for Radiation Biology and Medicine, Hiroshima University,
Hiroshima, Japan

T. Kawai · R. Nishikomori
Department of Pediatrics,
Kyoto University Graduate School of Medicine,
Kyoto, Japan

T. Sakaguchi
Department of Virology,
Hiroshima University Graduate School of Biomedical Sciences,
Hiroshima, Japan

Introduction

X-linked ectodermal dysplasia with immunodeficiency (XL-ED-ID) is an X-linked recessive disease which is characterized by missing or malformed teeth, coarse hair, dry skin, hypohidrosis, and immunodeficiency. It is reportedly caused by mutations in the inhibitor of a kappa light polypeptide gene enhancer in B cells, kinase gamma (*IKBKG*), also called nuclear factor-kappaB (NF-κB) essential modulator (*NEMO*) [1]. NEMO is a subunit of the inhibitor of kappaB (IκB) kinase (IKK) complex and plays pivotal regulatory roles in NF-κB signaling pathways. The IKK complex is activated via NEMO in response to stimulation of a wide range of receptors, including Toll like receptors, CD40, proinflammatory cytokine receptors, ectodysplasin receptor, and receptor activator of NF-κB [2–4]. The activated IKK complex induces ubiquitin-mediated proteasomal degradation of IκB, resulting in translocation of NF-κB dimers from the cytoplasm to the nucleus. Subsequently, NF-κB binds to specific κB sites and regulates target gene transcription, activating downstream

processes involved in inflammation, immunity, cell proliferation, apoptosis, ectodermal formation, and osteogenesis.

Patients with XL-ED-ID are susceptible to multiple and severe bacterial infections of the respiratory and gastrointestinal tracts, skin, soft tissues and bones, together with meningitis and septicemia, from the early stage of infancy [5, 6]. In addition to recurrent severe pyogenic infections, patients also show susceptibility to mycobacterial infections. Although viral infections are not thought to be representative symptoms, some patients suffer from viral infections, e.g., cytomegalovirus (CMV), molluscum contagiosum virus, human papilloma virus, and herpes simplex virus [6, 7]. The immunological abnormalities in the patient with XL-ED-ID are characterized by dysregulated immunoglobulin synthesis or hyperimmunogloblin M (hyper-IgM) syndrome, impaired specific antibody production, defective natural killer (NK) cell activity, and poor proinflammatory cytokine production in response to physiological stimuli. Thus, in patients with XL-ED-ID, responses to various stimuli such as lipopolysaccharide (LPS), interleukin-1 (IL-1), IL-12, IL-18, tumor necrosis factor alpha (TNF-α), and CD40 ligand (CD40L) are impaired [8–11].

Male subjects inheriting large deletions, frameshifts, or other amorphic mutations in *IKBKG* die in utero, indicating that NEMO is essential for development in humans. The mutations in patients with XL-ED-ID are hypomorphic and these mutations impair, but do not abolish NF-κB signaling, thus resulting in distinct clinical and immunological phenotypes.

We identified a novel splice-site mutation, 769−1 G>C, in *IKBKG* in a Japanese boy with XL-ED-ID. This splice-site mutation was shown to produce not only various types of abnormal messenger RNAs (mRNAs), but also low expression of wild-type (WT) mRNA. The expression of WT and abnormal NEMO proteins was also confirmed to be at decreased level in this patient. The decreased expression of NEMO protein is suspected to play an important role in the development of XL-ED-ID.

Methods

Case Report

The patient was a 12-year-old male. He presented with mild mental retardation, conical-shaped teeth, and hypodontia. Hypohidrosis and alopecia were not observed. Similar symptoms were not observed in his family members. He had suffered from recurrent bacterial infections, e.g., three episodes of bacterial meningitis (at 18, 27, and 28 months of age; the pathogenic bacteria isolated from cerebrospinal fluid was *Streptococcus pneumoniae* in the first and third episodes and was unknown in the second episode), recurrent episodes of pneumonia, cellulitis (at 4 years of age; the pathogenic bacteria was unidentified), left knee arthritis (8 years of age, *S. pneumoniae*), and osteomyelitis (12 years old; the pathogenic bacteria was unknown). Furthermore, the patient had also suffered from measles despite receiving a measles vaccination.

The white blood cell and neutrophil counts were both slightly decreased (Table I). The percentage of CD3, CD4, CD8, and CD16/56 in lymphocytes was within the normal range. However, a mild decrease was noted in the $CD19^+$ B cell population. The serum immunoglobulin levels and complement levels were within normal ranges. The production of specific antibodies against *S. pneumoniae* and measles were impaired despite having a history of infections and vaccinations. The specific antibody against *S. pneumoniae* was measured by ELISA and included the antigens of 23 serotypes. He had been vaccinated once with Pneumovax®23 at the age of 9. Furthermore, the specific antibody against the mumps virus was not produced, although the patient was administered the mumps vaccination. However, specific antibodies against CMV, Epstein–Barr virus, Varicella zoster virus, and rubella virus were normally developed. The abdominal ultrasonography examination revealed that the patient's spleen was of normal size. The parents of the patient did not present with immunodeficiency or incontinentia pigmenti.

We obtained blood samples from the patient and healthy adult controls after obtaining informed consent. This study was approved by the Ethics Committee/Internal Review Board of Hiroshima University.

Molecular Genetics

Total RNA was extracted from peripheral blood mononuclear cells (PBMCs). Subsequently, complementary DNA (cDNA) was synthesized by reverse transcription. Polymerase chain reaction (PCR) was performed using primer set 1 (which spans the entire coding region of *IKBKG*, see Supplementary Table) and an Expand Long PCR system (Roche Diagnostics, Germany). The PCR products were sequenced using primer sets 1 and 2. Genomic DNA was extracted from peripheral blood leukocytes and buccal mucosa. Sequence analysis was performed as described previously [12]. In order to investigate the splicing pattern of exon 7, PCR was performed using peripheral blood leukocyte cDNA and primer set 3. The PCR products were cloned into the pGEM-T Easy vector (Promega, USA), and individual alleles were sequenced.

To generate WT and mutant *IKBKG* plasmids, cDNA was synthesized from the patient's PBMCs. PCR was performed using KOD PCR system (TOYOBO, Japan) and primer set 4 (F and R), which includes *Hin*dIII and *Bam*HI sites at the 5′- and 3′-end, respectively, and eliminates the stop codon of *IKBKG*. The PCR products were cloned into the pGEM-

Table I Laboratory data

			RR			Negative range
Leukocyte fraction				Specific antibody		
WBC	5,390	/μl	6,000–10,000	*S. pneumoniae*	Negative	Negative
Neut	1,024	/μl	3,300–7,500	Measles	<8	<8
Ly	3,719	/μl	1,200–4,000	Rubella	>128	<2
Mo	215	/μl	200–950	VZV IgG	40	<10
Eo	377	/μl	0–600	Mumps	<2	<2
Lymphocyte fraction				JEV	<4	<4
CD3	72	%	52–78	CMV IgG	20	<4
CD19	5	%	8–24	EBV VCA IgG	20	<10
CD16/56	21	%	6–27	EBV VCA IgM	<10	<10
CD3/4	38	%	25–48	EBNA	<10	<10
CD3/8	19	%	9–35	Polio type 1, 2, 3	<4	<4
Immunobiochemistry				Pertussis	10	<10
IgG	966	mg/dl	816–1,342	Others		
IgA	292	mg/dl	154-336	NK cell cytotoxicity	6	15–40%
IgM	76	mg/dl	62-103	LTT	Positive	
IgE	54	mg/dl	<100			
CH50	31.2	U/ml	25–48			
C3	97	mg/dl	65–135			
C4	19	mg/dl	13–40			

VZV Varicella zoster virus, *JEV* Japanese encephalitis virus, *CMV* cytomegalovirus, *EBV* Epstein–Barr virus, *EBNA* EBV nuclear antigen, *LTT* lymphocyte transformation test, *RR* reference range

T Easy vector. To generate the construct with a frameshift mutation that produced a premature stop codon, we repeated the PCR to eliminate the original stop codon using primer set 4 (F and R2). These fragments were cloned into P3xFlag-CMV-14 expression vector (Invitrogen, USA) using the *Hin*dIII and *Bam*HI sites.

Reporter Assay

WT and mutant constructs (2 ng per well), IgK-cona-Luc (provided by S. Yamaoka), and pRL-TK (TOYO-B-Net, Japan) were transfected into the NEMO null rat fibroblast cells (provided by S. Yamaoka) using FuGENE HD Transfection Reagent (Roche). We used WT and each of the mutants (1 ng per well, respectively) for co-transfection experiments. At 24 h after transfection, the cells were stimulated with 15 ng/ml LPS (Sigma-Aldrich, USA) for 4 h. Then, cells were subjected to a luciferase assay using the PicaGene Dual Luciferase Assay Kit (TOYO-B-NET). Experiments were done in triplicate and the firefly luciferase activity was normalized to the renilla activity.

Western Blot Analysis

The total proteins from EB virus-transformed B cells (EBV-B cells) were subjected to an immunoblot analysis. We used a mouse anti-NEMO antibody (BD Bioscience, USA) and an anti-flag antibody (Sigma-Aldrich) to detect the NEMO protein and an anti-β-actin antibody (Sigma-Aldrich) as a loading control.

Electrophoretic Mobility Shift Assay

EBV-B cells were stimulated with 10 ng/ml IL-1β (Sigma-Aldrich) for 30 min and subjected to nuclear extraction. We incubated 10 μg of nuclear extract with ^{32}P-labeled (α-dATP) NF-κB probe. The NF-κB double-stranded oligonucleotides corresponding to a NF-κB-binding site consensus sequence 5′-GAT CAT GGG GAA TCC CCA-3′ were used as a NF-κB probe [13].

Flow Cytometry and Carboxyfluorescein Diacetate Succinimidyl Ester Analyses

Flow cytometry analysis of intracellular NEMO protein was performed using the previously reported method [12]. The cells were stained for the following lineage markers after staining for NEMO: CD3, CD14, CD19, and CD56 (BD Bioscience). For CD40L stimulation, PBMCs were cultured with recombinant soluble human CD40L (rCD40L; 2.5 μg/ml; PeproTech Inc, USA) for 48 h and then stained for FCE2 (CD23), ICAM-1 (CD54), Fas (CD95), and CD19

(BD Bioscience). For memory B cell analysis, PBMCs were stained with APC-conjugated anti-CD19, PE-conjugated anti-CD27, and FITC-conjugated anti-IgD antibodies (BD Biosciences). Three-color analysis was carried out by gating on CD19-APC-positive B cells.

For the preparation of measles virus-infected cell lysates (measles lysates), Vero cells were infected with measles virus (the Edmonston strain). Measles lysates were prepared from the cells by clarification with a low-speed centrifugation. The PBMCs from the patient and five healthy adult controls (all were approximately 20 years of age and had developed specific antibodies against measles, rubella, and mumps) were incubated with carboxyfluorescein diacetate succinimidyl ester (CFSE) (Sigma-Aldrich) at a concentration of 0.05 mM [14, 15]. The cells were cultured for 7 days in RPMI-1640 (Sigma-Aldrich) containing 10% AB human serum supplemented with 1 or 3 μg/ml phytohemagglutinin (PHA) (Sigma-Aldrich), 1 or 10 μg/ml measles lysates, 1 or 5 μg/ml rubella lysates (Meridian Life Science, USA), and 1 or 10 μg/ml mumps lysate (Fitzgerald, USA). These cells were stained with APC-conjugated anti-CD4 antibodies (BD Biosciences) and subjected to a flow cytometry analysis.

Cytokine Measurements

We used PBMCs from the patient and four age-matched healthy adult controls (aged 20 years). $CD14^+$ cells were purified from PBMCs using by magnetic sorting (BD Biosciences). The purity levels of $CD14^+$ cells were more than 90%. The $CD14^+$ cells were cultured for 48 h with the addition of 100 U/ml LPS, and the concentration of TNF-α in supernatant was measured in duplicate by Luminex.

Results

A Novel Splice-Site Mutation in *IKBKG* Results in Various Abnormal Splicing Products

High molecular weight DNA was extracted from both the peripheral blood samples and buccal mucosa, and the exons and flanking introns of *IKBKG* were amplified by PCR and sequenced. We identified a novel hemizygous single base-pair G-to-C substitution at nucleotide 769 (−1), 769−1 G>C, of intron 6 in *IKBKG* in the peripheral blood samples (Fig. 1a). The same mutation was also identified in genomic DNA from buccal mucosa, suggesting that this mutation is a germ-line mutation (data not shown). We could not examine the patient's parents and siblings because we could not obtain consent from these family members. Thus, we excluded the possibility that this mutation was a common or irrelevant polymorphism by sequencing 214 healthy

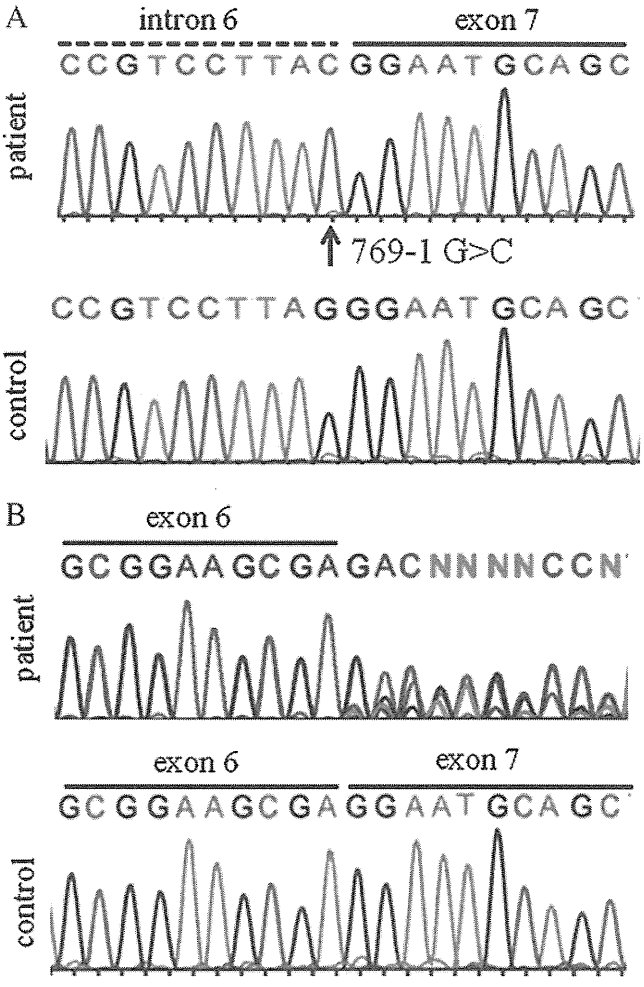

Fig. 1 Sequence analysis. **a** Genomic DNA from the patient and healthy controls were amplified by PCR and the products were analyzed by Sanger sequencing. A novel hemizygous single base-pair G-to-C substitution at nucleotide 769 (−1), 769−1 G>C, was identified in IVS6 of *IKBKG*. **b** Total RNA was extracted from peripheral blood mononuclear cells and cDNA was synthesized by reverse transcription. PCR was performed using primers that spanned the entire coding region of *IKBKG*. The presence of various abnormal splicing variants was predicted in the patient

individuals, including 58 Japanese individuals. A splice junction sequence is highly conserved in eukaryotic cells, which is generally known as a GT-AG rule [16, 17]. Since 769−1 G>C is involved in the highly conserved splicing acceptor site, we analyzed the impact of this mutation on NEMO mRNA splicing. As shown in Fig. 1b, the presence of various abnormal splicing variants was predicted.

In order to investigate the effect of this mutation on splicing, we performed PCR on cDNA with primers which span exons 6 and 7 of *IKBKG*. PCR products were cloned into pGEM-T Easy vector and were subjected to sequence analysis. A sequence analysis of 24 clones demonstrated that 7 clones were derived from normal splicing and the other 17 clones from various abnormal splicing events

(Fig. 2a). Although these abnormal splicing patterns contained insertions and/or deletions in various locations, the major mutant patterns were a 171-bp insertion (+171-NEMO) and 64-bp insertion (+64-NEMO) at the splice acceptor site of exon 7. Among the 17 clones from the abnormal splicing, 13 clones had in-frame changes resulting in large conformational changes of the NEMO protein, and 4 clones (+64-NEMO) were a frameshift change resulting in the premature termination of protein translation (Fig. 2a). The ratio of WT and mutants was similar in PHA- and IL-2-induced T cell blasts which were obtained on the same day (Fig. 2b). We also collected blood samples from the patient on other days, including 1 day the patient was experiencing fever. The ratio of WT to mutant differed in these later samples, compared to those in the initial analysis. In these later timepoints, the ratio of WT was decreased to 5% or 18%, suggesting that the ratio of WT mRNA varies in the patient over time (Fig. 2c, d). To examine whether these splicing variants were also observed in healthy individuals, we tested five healthy individuals and did not find any of the variants found in the patient (representative sequences are shown in Fig. 1b). Altogether, these results suggest that the 769−1 G>C mutation in *IKBKG* is responsible for various abnormal NEMO splicing products.

NEMO Protein Expression Is Decreased in the Patient

In order to examine the effect of the *IKBKG* mutation at the protein level, we analyzed the expression of intracellular NEMO by a flow cytometry analysis. The expression of the NEMO protein in the patient was lower than that in healthy controls in terms of CD3, CD4, CD8, CD56, CD14, and CD19-positive cells (Fig. 3a). Next, we performed an

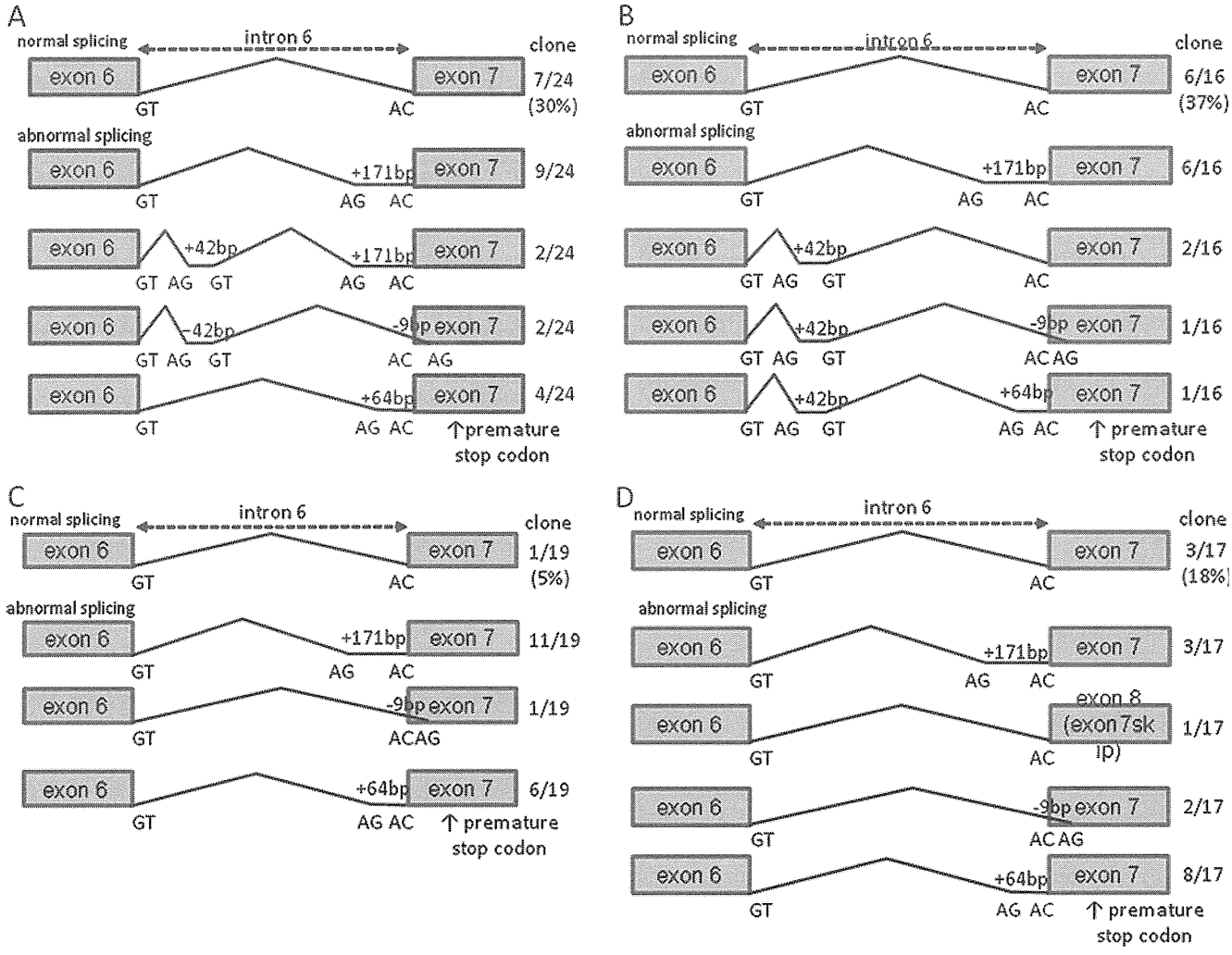

Fig. 2 Cloning analysis. **a** PCR products were cloned into the pGEM-T Easy vector and were subjected to sequence analysis. The splice pattern and the observed number of each clone are shown. The same studies were performed using PHA- and IL-2-induced T cell blasts which were obtained the same day (**b**), PBMCs obtained another day (**c**), and PBMCs obtained on the day the patient was experiencing fever (**d**). The splice pattern and the ratio of WT or mutant variants were different based on the timing of blood collection

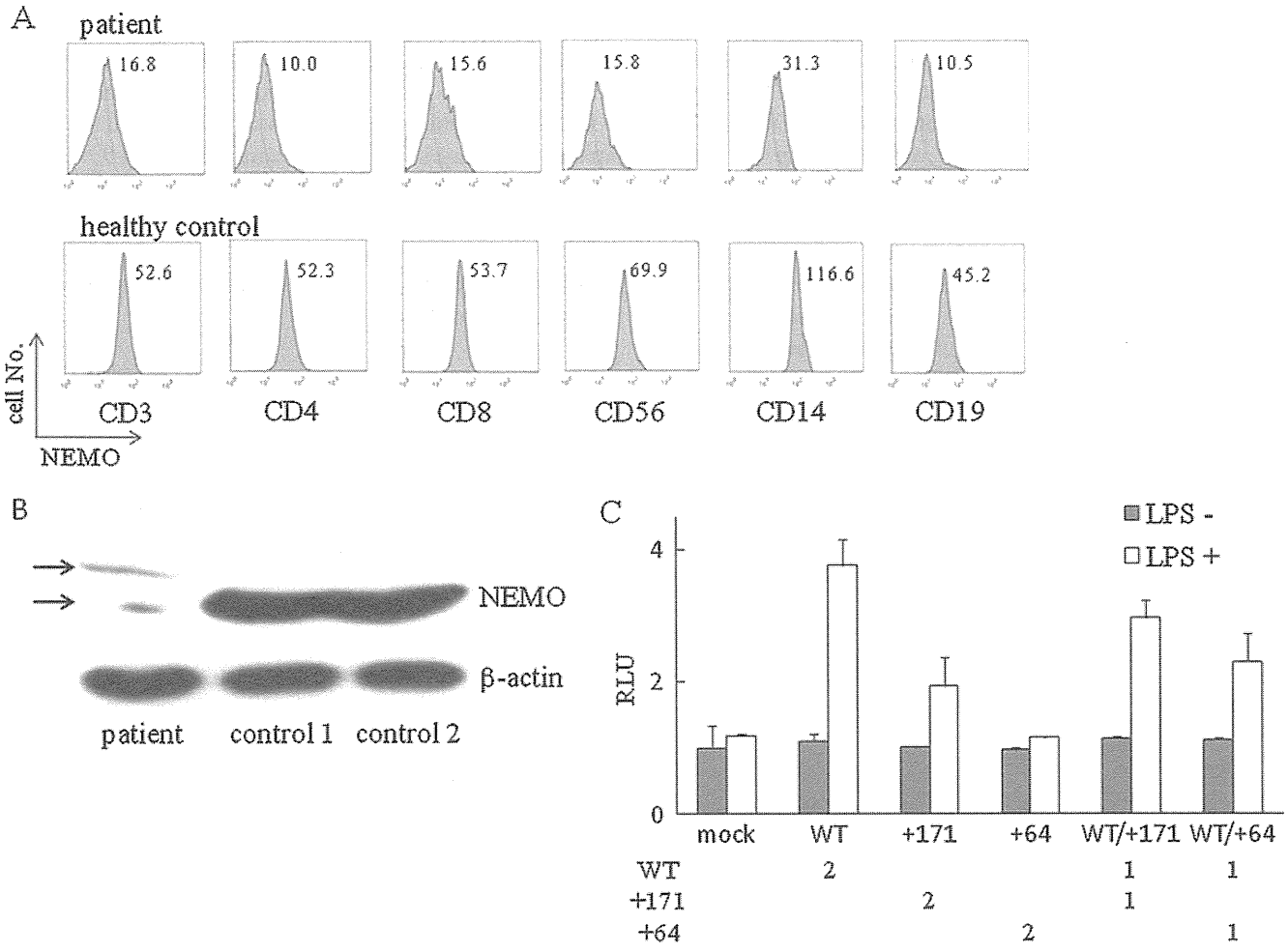

Fig. 3 Analysis of NEMO protein expression and reporter assay. **a** Expression of intracellular NEMO protein from the patient was decreased in various lineages of leukocytes. The geometrical mean fluorescence intensity of NEMO is shown in the FACS profile. **b** EBV-B cells from the patient showed decreased levels of NEMO protein expression. The *upper arrow* shows the band derived from +171-NEMO (approximately 57 kDa), while the *lower arrow* shows WT-NEMO (50 kDa). EBV-B cells in the patient were established from the same blood collection as was used for the cloning analysis of Fig. 2a. **c** WT-, +171-, and +64-NEMO were transfected into NEMO null cells, and NF-κB activity was measured by luciferase assay. The quantity of plasmids (nanogram) used for transfection is described

immunoblot analysis using EBV-B cells from the patient. As shown in Fig. 3b, two major bands were detected, corresponding to the expected molecular weight of the +171-NEMO mutant (approximately 57 kDa) and the known molecular weight of WT-NEMO (50 kDa). The results of densitometry revealed that the expression of WT-NEMO protein from the patient was eightfold lower than that from healthy controls. NEMO mutant proteins derived from other abnormally spliced mRNAs were not detected in this assay.

The Mutant NEMO Proteins Show Decreased NF-κB Transcriptional Activity

To further clarify the characteristics of these abnormally spliced mRNAs, we performed transient gene expression experiments specifically focused on the abnormal splicing products, +171- and +64-NEMO. WT and these mutant constructs were transfected into NEMO null cells. The expression of the WT- and +171-NEMO proteins was detected by either anti-NEMO or anti-Flag antibodies (Supplementary Figure). We were unable to detect the expression of the +64-NEMO protein in the transfectants, suggesting that the +64-NEMO protein may be unstable. Then, we examined the impact of these mutants on NF-κB activation using reporter assay. As shown in Fig. 3c, +64-NEMO abolished NF-κB activation in response to LPS stimulation. On the other hand, +171-NEMO displayed residual NF-κB activity. To further clarify the effect of these mutants on the WT protein, we performed a co-transfection experiment. Co-transfection with half of the amount of WT and +171-NEMO (WT/+171) resulted in only 75% of the

NF-κB activity compared to cells transfected with WT-NEMO, while co-transfection with WT and +64-NEMO (WT/+64) resulted in approximately 50% of WT activity. Considering that +64-NEMO is not expressed at the protein level, the 50% NF-κB activity observed here is likely derived from half the amount of WT-NEMO plasmid. On the other hand, +171-NEMO is thought to have residual activity, even after co-transfection with WT-NEMO. This result suggests that these mutants do not seem to exert a dominant-negative effect against WT-NEMO-mediated NF-κB activation. However, we could not completely rule out the negative effect caused by the other abnormally spliced variants, since we examined only two representative variants.

The Functional Activity via NEMO Is Impaired in the Patient

To analyze the functional impairment caused by the NEMO mutation, we examined the CD23, CD56, and CD95 expression on $CD19^+$ B cells, markers of activated B cells, in response to CD40L stimulation. As shown in Fig. 4a, CD54 and CD95 expressions were reduced compared to healthy controls, and CD23 expression was not detected in the patient's B cells, suggesting that activation of B cells was not completely abrogated in the patient, but instead $CD19^+$ B cells from the patient showed weak levels of activation. Therefore, the patient's cells showed partial, but not complete, impairment following CD40L stimulation. Next, we tested TNF-α production in response to LPS stimulation in peripheral blood $CD14^+$ monocytes. As shown in Fig. 4b, $CD14^+$ monocytes from the patient showed a lower level of TNF-α production compared with those from healthy controls. To further clarify the functional defects, we assessed NF-κB DNA-binding ability in response to IL-1β stimulation using EBV-B cells. As shown in Fig. 4c, NF-κB DNA-binding ability was severely impaired, but not abolished, in the patient. Thus, similar to other patients with XL-ED-ID, the patient's cells also showed impairment in response to various stimuli which induce IKK activation.

Memory B Cells Are Decreased in the Patient

The number of $CD27^+$ memory B cells within the $CD19^+$ B cell population was decreased in the patient (6.0%) in comparison to the number observed in healthy controls (30.4±17.8%, $n=10$). A reduced number of $CD27^+$ memory B cells has also been reported in patients with X-linked anhidrotic ectodermal dysplasia with hyper-IgM syndrome (HED-ID) caused by NEMO impairment [18, 19] as well as in a patient with a 5′ untranslated region (UTR) mutation of *IKBKG*, with high levels of IgA [20]. However, as far as we know, a reduction in the memory B cell compartment has not yet been reported in patients with ED-ID. B cells in patients with defect in NF-κB are unable to undergo somatic hypermutation and class switch recombination, resulting in a loss of memory B cells [19, 21, 22]. Although we need to test other patients with ED-ID to confirm this memory B cell phenotype, the diminished memory B cell population may become a common finding not only in patients with HED-ID, but also in patients with an impairment of NEMO.

The Increase in $CD4^+$ T Cell Proliferation Is Impaired for Measles and Mumps Infections

The patient developed measles in spite of having a history of measles vaccination. Furthermore, although specific antibodies against measles and mumps virus were not detected, specific antibodies against CMV, Epstein–Barr virus, Varicella zoster virus, and rubella virus were normal. To clarify the mechanism underlying the impairment of specific antibody production against measles and mumps viruses, we tested the specific T cell response against these viral infections. We analyzed $CD4^+$ T cells using a CFSE proliferation assay according to the method described in a previous report [23]. $CD4^+$ T cells from the patient were unable to proliferate in response to measles lysate and mumps lysate (Fig. 5a, b). On the other hand, they proliferated well in response to PHA and rubella lysate. CFSE is a commonly used and useful tool for analyzing specific T cell response against *Candida*, CMV, measles viruses, and others, and these results suggest that the specific T cell response against measles and mumps virus is impaired in the patient [14, 15, 23]. These findings were compatible with patient's laboratory findings of the impairment of a specific antibody production against measles virus and mumps virus, in spite of having received these vaccinations and having a prior measles infection.

Discussion

We identified a novel hemizygous splice-site mutation in *IKBKG* in a Japanese boy with XL-ED-ID. Both the WT and various abnormally spliced forms of NEMO mRNA were observed in the patient's cells. There are two possibilities which may account for this finding. One is leakage through the splice-site mutation, the other is mosaicism. Leakage through the splice-site mutation has also been described in many human diseases [24–26], including in a patient with a NEMO abnormality who had a splice-site mutation, 1056−1 G>A [27]. Similar to what was observed in our current study, the ratio of WT to mutant NEMO mRNA observed varied with the timing of blood

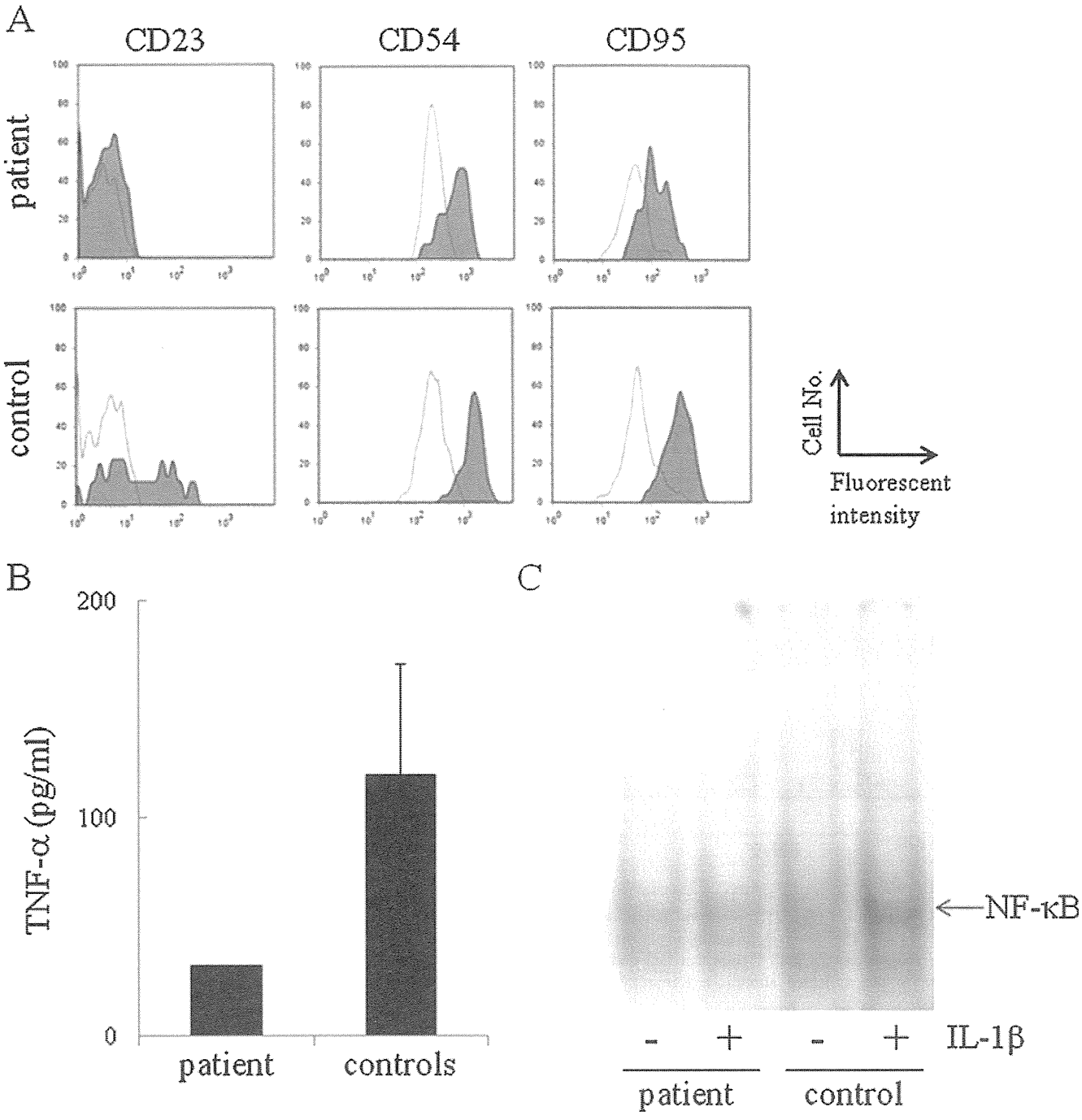

Fig. 4 Analysis of functional activity via NEMO. **a** Expression of CD23, CD54, and CD95, the surface markers of activated B cells, was measured using flow cytometry. PBMCs from the patient and healthy controls were treated with (*shaded histograms*) or without (*open histograms*) CD40L. **b** TNF-α production in response to LPS by $CD14^+$ cells was measured by Luminex. Data from the healthy subjects are represented as mean ± SD (n=4). **c** The NF-κB DNA-binding ability in response to IL-1β was measured by electrophoretic mobility shift assay. EBV-B cells from the patient showed a lower level of DNA-binding ability than healthy controls

collection in the patient with a 1056−1 G>A mutation. Curiously, however, there is a difference between the expression of WT-NEMO protein and the frequency of WT-NEMO mRNA in our patient. Although the frequency of WT-NEMO mRNA observed in the patient in our splicing assay was approximately 30% of all splice transcripts, expression of NEMO protein from the patient was only 12.5% that of WT levels. We suspect that the influence of nonsense-mediated RNA decay can explain this inconsistency between WT-NEMO expression at the mRNA and protein level. Some abnormally spliced forms of NEMO, such as 64-NEMO, result in premature stop codon. These

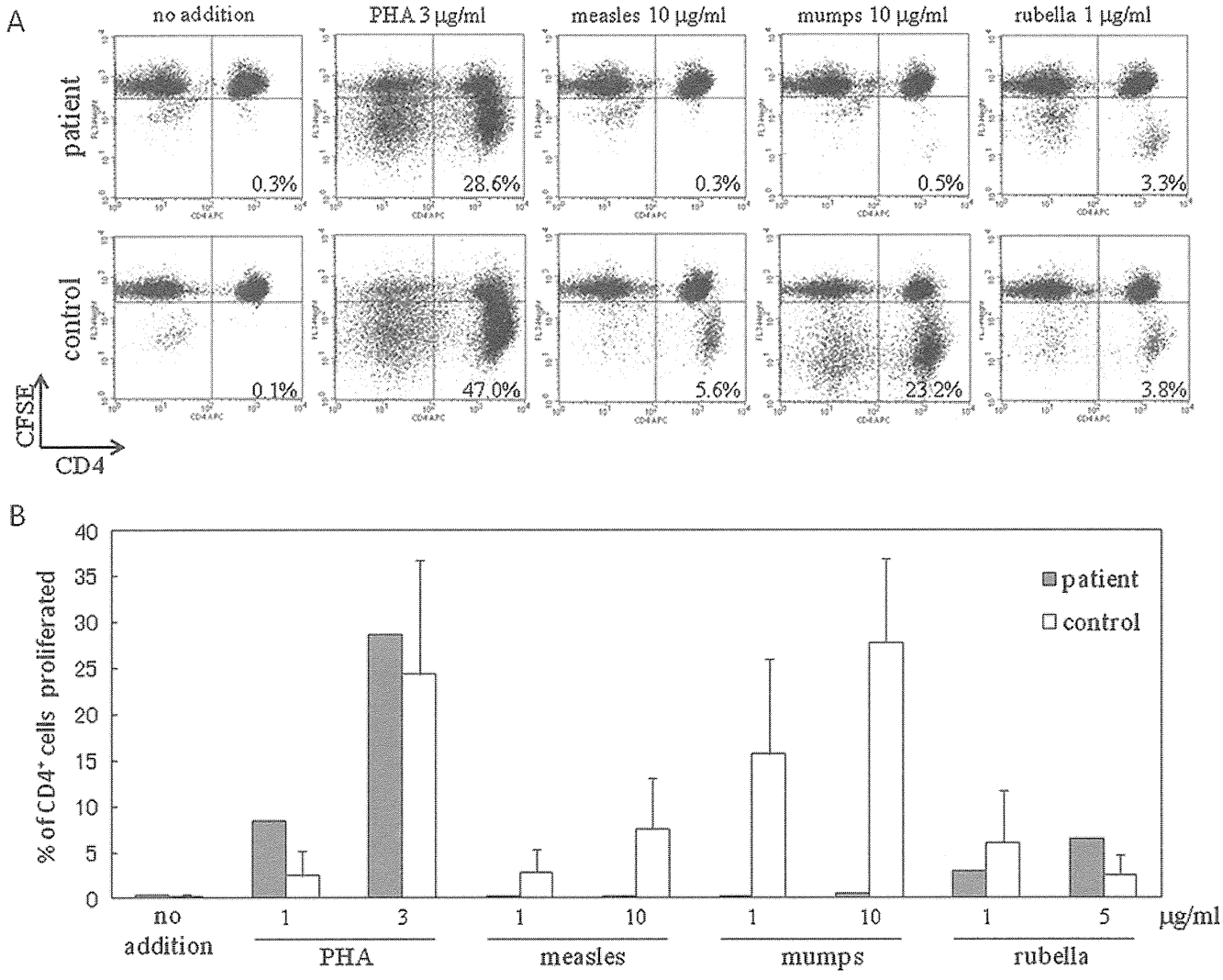

Fig. 5 CFSE analysis of the response of $CD4^+$ cells to PHA and various viruses. **a** Representative FACS figures from the patient and healthy subjects are shown. The *lower-right quadrant* of the FACS profile indicates the proportion of $CD4^+$ T cells that had undergone division in response to the indicated stimuli. **b** Summary of the percentage of proliferating $CD4^+$ T cells is shown. The data in the *white columns* represent the mean ± SD of five healthy subjects. Although $CD4^+$ T cells from the patient proliferated in response to the rubella virus, few divided cells were observed upon stimulation with the measles or mumps viruses

products are predicted to be susceptible to nonsense-mediated RNA decay. Therefore, although the splicing assay in this study is an effective way to detect variously spliced transcripts derived from the 769−1 G>C mutation, it may overestimate the proportion of in-frame transcripts which include WT-NEMO.

The other possibility to explain the existence of both WT and mutant mRNAs is germ-line or reversion mosaicism of WT and mutant NEMO-containing cells, as has previously been reported in patients with immunological disorders [28–31]. Furthermore, a reversion mosaicism has been identified in one patient with XL-ED-ID [12]. This patient exhibited NEMO protein expression that varied among cell lineages. Two types of NEMO-expressing cells, NEMO high and NEMO low, were observed by flow cytometric analysis. However, the pattern of NEMO expression did not differ among the lineages in our current study (Fig. 3a). In addition, we did not identify the WT-NEMO sequence from Sanger sequence using genomic DNA extracted from peripheral blood leukocytes or buccal mucosa from the patient (Fig. 1a). Taken together, although we could not completely exclude the possibility of low frequency mosaicism, we presume that normal NEMO mRNAs are derived from leakage through the splice-site mutation that may give rise to XL-ED-ID.

The levels of NEMO protein expression decreased markedly, and the functional activity via NEMO in response to various stimuli were impaired in our patient. Recently, Mooster et al. reported a patient with immunodeficiency caused by a splice-site mutation in the 5′ UTR of the

IKBKG [20]. This patient also showed decreased expression of the NEMO protein, thus resulting in reduced NF-κB activity. In addition, the authors proposed that inadequate levels of normal NEMO protein played a role in the molecular pathogenesis of this patient. Similarly, decreased expression of NEMO protein was also suspected to have played an important role in the clinical manifestations of our patient. However, in contrast to our patient, neither the patients with 1056−1 G>C nor 5′ UTR mutation that demonstrated a residual expression of WT-NEMO presented with ectodermal dysplasia. Further studies will therefore be required to elucidate the factor that is associated with the development of the ectodermal phenotype.

$CD4^+$ T cells from the patient exhibit impaired proliferation in response to measles and mumps viruses. On the other hand, normal proliferation was observed upon stimulation with the rubella virus. To our knowledge, this is the first study to clarify an impairment of T cell proliferation in response to viral infections by CSFE analysis in a patient with NEMO mutation. These results were completely consistent with the laboratory finding of specific antibody production against rubella, but not measles and mumps viruses. Furthermore, the impairment of antibody production against measles, but not rubella, was also observed in another patient with ED-ID carrying a D311E hypomorphic mutation in *NEMO* (Imai et al., in revision in J Clin Immunol). It is interesting to speculate how the impairment of the NEMO protein disturbs the response against measles. Generally, the first line of host defense against viral infection is the innate immune system [32]. Viral infections induce inflammatory reactions via induction of IFNs and via the activation of NF-κB. The activation of interferon regulatory factor-3 (IRF-3) plays an important role in the induction of IFNs against viral infections. IRF-3 recognizes the measles virus nucleocapsid and triggers the induction of interferon production. However, IRF-3 activation and IRF-3-dependent gene induction are abrogated in NEMO-deficient cells [33]. Indeed, impairment of TLR3-induced NF-κB- and IRF-3-dependent IFN induction has also been documented in a patient with NEMO mutation (Audry et al. J Allergy Clin Immunol. in press, reference number: YMAI 8998). In addition, the activation of NF-κB also plays a pivotal role in the host defense against measles. The measles virus phosphoprotein upregulates the ubiquitin-modifying enzyme A20, a negative feedback regulator of NF-κB, resulting in viral escape from the host immune system [34, 35]. Therefore, the impairments of acquired immunity against viral infections observed in the patient may be derived from an impairment of innate immunity caused by NEMO mutation. Further studies will therefore be required to confirm the clinical and cellular phenotype against viral infections in other patients with NEMO mutation.

Conclusion

The 769−1 G>C mutation was shown to cause a decrease in NF-κB activation through the decreased expression level of NEMO protein, thus resulting in the development of XL-ED-ID.

Acknowledgments This work was supported by a Grant-in-Aid for Young Scientist (B) No. 20790731 from Japan Society for the Promotion of Science. This work was also supported by the grants from the Japanese Ministry of Education, Culture, Sports, and Technology and grants from the Japanese Ministry of Health, Labor, and Welfare. We wish to thank the Analysis Center of Life Science, Hiroshima University for the use of their facilities. We also thank Natsuki Nabe and Yuki Takaoka for their valuable help with the reporter assay.

References

1. Doffinger R, Smahi A, Bessia C, Geissmann F, Feinberg J, Durandy A, et al. X-linked anhidrotic ectodermal dysplasia with immunodeficiency is caused by impaired NF-kappaB signaling. Nat Genet. 2001;27:277–85.
2. Fusco F, Pescatore A, Bal E, Ghoul A, Paciolla M, Lioi MB, et al. Alterations of the IKBKG locus and diseases: an update and a report of 13 novel mutations. Hum Mutat. 2008;29:595–604.
3. Puel A, Picard C, Ku CL, Smahi A, Casanova JL. Inherited disorders of NF-kappaB-mediated immunity in man. Curr Opin Immunol. 2004;16:34–41.
4. Courtois G, Smahi A, Israel A. NEMO/IKK gamma: linking NF-kappa B to human disease. Trends Mol Med. 2001;7:427–30.
5. Hanson EP, Monaco-Shawver L, Solt LA, Madge LA, Banerjee PP, May MJ, et al. Hypomorphic nuclear factor-kappaB essential modulator mutation database and reconstitution system identifies phenotypic and immunologic diversity. J Allergy Clin Immunol. 2008;122:1169–77.
6. Orange JS, Jain A, Ballas ZK, Schneider LC, Geha RS, Bonilla FA. The presentation and natural history of immunodeficiency caused by nuclear factor kappaB essential modulator mutation. J Allergy Clin Immunol. 2004;113:725–33.
7. Lee WI, Torgerson TR, Schumacher MJ, Yel L, Zhu Q, Ochs HD. Molecular analysis of a large cohort of patients with the hyper immunoglobulin M (IgM) syndrome. Blood. 2005;105:1881–90.
8. Filipe-Santos O, Bustamante J, Haverkamp MH, Vinolo E, Ku CL, Puel A, et al. X-linked susceptibility to mycobacteria is caused by mutations in NEMO impairing CD40-dependent IL-12 production. J Exp Med. 2006;203:1745–59.
9. Orange JS, Brodeur SR, Jain A, Bonilla FA, Schneider LC, Kretschmer R, et al. Deficient natural killer cell cytotoxicity in patients with IKK-gamma/NEMO mutations. J Clin Invest. 2002;109(11):1501–9.
10. Vinolo E, Sebban H, Chaffotte A, Israel A, Courtois G, Veron M, et al. A point mutation in NEMO associated with anhidrotic ectodermal dysplasia with immunodeficiency pathology results in destabilization of the oligomer and reduces lipopolysaccharide- and tumor necrosis factor-mediated NF-kappa B activation. J Biol Chem. 2006;281:6334–48.
11. Smahi A, Courtois G, Rabia SH, Doffinger R, Bodemer C, Munnich A, et al. The NF-kappaB signalling pathway in human diseases: from incontinentia pigmenti to ectodermal dysplasias and immune-deficiency syndromes. Hum Mol Genet. 2002;11:2371–5.

12. Nishikomori R, Akutagawa H, Maruyama K, Nakata-Hizume M, Ohmori K, Mizuno K, et al. X-linked ectodermal dysplasia and immunodeficiency caused by reversion mosaicism of NEMO reveals a critical role for NEMO in human T-cell development and/or survival. Blood. 2004;103:4565–72.
13. Puel A, Reichenbach J, Bustamante J, Ku CL, Feinberg J, Doffinger R, et al. The NEMO mutation creating the most-upstream premature stop codon is hypomorphic because of a reinitiation of translation. Am J Hum Genet. 2006;78:691–701.
14. Fazekas de St Groth B, Smith AL, Koh WP, Girgis L, Cook MC, Bertolino P. Carboxyfluorescein diacetate succinimidyl ester and the virgin lymphocyte: a marriage made in heaven. Immunol Cell Biol. 1999;77:530–8.
15. Lyons AB. Analysing cell division in vivo and in vitro using flow cytometric measurement of CFSE dye dilution. J Immunol Methods. 2000;243:147–54.
16. Mount SM. A catalogue of splice junction sequences. Nucleic Acids Res. 1982;10:459–72.
17. Mount SM. Genomic sequence, splicing, and gene annotation. Am J Hum Genet. 2000;67:788–92.
18. Jain A, Ma CA, Liu S, Brown M, Cohen J, Strober W. Specific missense mutations in NEMO result in hyper-IgM syndrome with hypohydrotic ectodermal dysplasia. Nat Immunol. 2001;2:223–8.
19. Jain A, Ma CA, Lopez-Granados E, Means G, Brady W, Orange JS, et al. Specific NEMO mutations impair CD40-mediated c-Rel activation and B cell terminal differentiation. J Clin Invest. 2004;114:1593–602.
20. Mooster JL, Cancrini C, Simonetti A, Rossi P, Di Matteo G, Romiti ML, et al. Immune deficiency caused by impaired expression of nuclear factor-kappaB essential modifier (NEMO) because of a mutation in the 5′ untranslated region of the NEMO gene. J Allergy Clin Immunol. 2010;126:127–32.
21. Kouskoff V, Nemazee D. Role of receptor editing and revision in shaping the B and T lymphocyte repertoire. Life Sci. 2001;69:1105–13.
22. Souto-Carneiro MM, Fritsch R, Sepulveda N, Lagareiro MJ, Morgado N, Longo NS, et al. The NF-kappaB canonical pathway is involved in the control of the exonucleolytic processing of coding ends during V(D)J recombination. J Immunol. 2008;180:1040–9.
23. Munier CM, Zaunders JJ, Ip S, Cooper DA, Kelleher AD. A culture amplified multi-parametric intracellular cytokine assay (CAMP-ICC) for enhanced detection of antigen specific T-cell responses. J Immunol Methods. 2009;345:1–16.
24. Arredondo-Vega FX, Santisteban I, Kelly S, Schlossman CM, Umetsu DT, Hershfield MS. Correct splicing despite mutation of the invariant first nucleotide of a 5′ splice site: a possible basis for disparate clinical phenotypes in siblings with adenosine deaminase deficiency. Am J Hum Genet. 1994;54:820–30.
25. Krawczak M, Reiss J, Cooper DN. The mutational spectrum of single base-pair substitutions in mRNA splice junctions of human genes: causes and consequences. Hum Genet. 1992;90:41–54.
26. Seyama K, Nonoyama S, Gangsaas I, Hollenbaugh D, Pabst HF, Aruffo A, et al. Mutations of the CD40 ligand gene and its effect on CD40 ligand expression in patients with X-linked hyper IgM syndrome. Blood. 1998;92:2421–34.
27. Orange JS, Levy O, Brodeur SR, Krzewski K, Roy RM, Niemela JE, et al. Human nuclear factor kappa B essential modulator mutation can result in immunodeficiency without ectodermal dysplasia. J Allergy Clin Immunol. 2004;114:650–6.
28. Arveiler B, de Saint-Basile G, Fischer A, Griscelli C, Mandel JL. Germ-line mosaicism simulates genetic heterogeneity in Wiskott–Aldrich syndrome. Am J Hum Genet. 1990;46:906–11.
29. Hirschhorn R, Yang DR, Puck JM, Huie ML, Jiang CK, Kurlandsky LE. Spontaneous in vivo reversion to normal of an inherited mutation in a patient with adenosine deaminase deficiency. Nat Genet. 1996;13:290–5.
30. Wada T, Schurman SH, Otsu M, Garabedian EK, Ochs HD, Nelson DL, et al. Somatic mosaicism in Wiskott–Aldrich syndrome suggests in vivo reversion by a DNA slippage mechanism. Proc Natl Acad Sci U S A. 2001;98:8697–702.
31. Stephan V, Wahn V, Le Deist F, Dirksen U, Broker B, Muller-Fleckenstein I, et al. Atypical X-linked severe combined immunodeficiency due to possible spontaneous reversion of the genetic defect in T cells. N Engl J Med. 1996;335:1563–7.
32. Yokota S, Okabayashi T, Fujii N. The battle between virus and host: modulation of Toll-like receptor signaling pathways by virus infection. Mediators Inflamm. 2010;2010:184328.
33. Zhao T, Yang L, Sun Q, Arguello M, Ballard DW, Hiscott J, et al. The NEMO adaptor bridges the nuclear factor-kappaB and interferon regulatory factor signaling pathways. Nat Immunol. 2007;8:592–600.
34. Indoh T, Yokota S, Okabayashi T, Yokosawa N, Fujii N. Suppression of NF-kappaB and AP-1 activation in monocytic cells persistently infected with measles virus. Virology. 2007;361:294–303.
35. Yokota S, Okabayashi T, Yokosawa N, Fujii N. Measles virus P protein suppresses Toll-like receptor signal through up-regulation of ubiquitin-modifying enzyme A20. FASEB J. 2008;22:74–83.

J Clin Immunol (2012) 32:39–49
DOI 10.1007/s10875-011-9600-0

Successful Treatment with Infliximab for Inflammatory Colitis in a Patient with X-linked Anhidrotic Ectodermal Dysplasia with Immunodeficiency

Tomoyuki Mizukami · Megumi Obara · Ryuta Nishikomori · Tomoki Kawai · Yoshihiro Tahara · Naoki Sameshima · Kousuke Marutsuka · Hiroshi Nakase · Nobuhiro Kimura · Toshio Heike · Hiroyuki Nunoi

Received: 23 July 2011 / Accepted: 15 September 2011 / Published online: 13 October 2011

Abstract X-linked anhidrotic ectodermal dysplasia with immunodeficiency (X-EDA-ID) is caused by hypomorphic mutations in the gene encoding nuclear factor-κB essential modulator protein (NEMO). Patients are susceptibile to diverse pathogens due to insufficient cytokine and frequently show severe chronic colitis. An 11-year-old boy with X-EDA-ID was hospitalized with autoimmune symptoms and severe chronic colitis which had been refractory to immunosuppressive drugs. Since tumor necrosis factor (TNF) α is responsible for the pathogenesis of NEMO colitis according to intestinal NEMO and additional TNFR1 knockout mice studies, and high levels of TNFα-producing mononuclear cells were detected in the patient due to the unexpected gene reversion mosaicism of NEMO, an anti-TNFα monoclonal antibody was administered to ameliorate his abdominal symptoms. Repeated administrations improved his colonoscopic findings as well as his dry skin along with a reduction of TNFα-expressing T cells. These findings suggest TNF blockade therapy is of value for refractory NEMO colitis with gene reversion.

Keywords NEMO colitis · infliximab · gene reversion

Introduction

X-linked anhidrotic ectodermal dysplasia with immunodeficiency (X-EDA-ID) is a rare inherited disease caused by hypomorphic mutations in the gene encoding nuclear factor-κB

Electronic supplementary material The online version of this article (doi:10.1007/s10875-011-9600-0) contains supplementary material, which is available to authorized users.

T. Mizukami · M. Obara · H. Nunoi (✉)
Division of Pediatrics, Department of Reproductive and Developmental Medicine, Faculty of Medicine, University of Miyazaki,
5200 Kihara, Kiyotake,
Miyazaki 889-1692, Japan
e-mail: h-nunoi@fc.miyazaki-u.ac.jp

T. Mizukami
Kumamoto Saishunso National Hospital,
Kumamoto, Japan

R. Nishikomori · T. Kawai · T. Heike
Department of Pediatrics,
Kyoto University Graduate School of Medicine,
Kyoto, Japan

Y. Tahara
Department of Gastroenterology and Hematology,
Faculty of Medicine, University of Miyazaki,
Miyazaki, Japan

N. Sameshima · K. Marutsuka
Department of Pathophysiology, Faculty of Medicine,
University of Miyazaki,
Miyazaki, Japan

H. Nakase
Department of Gastroenterology and Hepatology,
Kyoto University Graduate School of Medicine,
Kyoto, Japan

N. Kimura
Division of Medical Oncology, Hematology and Infectious Disease, Department of Medicine, Fukuoka University,
Fukuoka, Japan

(NF-κB) essential modulator (NEMO), which is the regulatory subunit of IκB kinase [1–3]. Mutations of NEMO can cause an impaired capacity to activate NF-κB, resulting in defects in ectodermal differentiation and innate and adaptive immunity [4, 5]. Affected patients generally show multiple developmental anomalies in ectodermal tissues such as sparse hair, hypodontia with conical teeth, and anhidrosis or hypohidrosis due to lack of sweat glands. These patients also suffer from severe life-threatening infections in various sites caused by Gram-positive or Gram-negative bacteria or mycobacteria. Immunological abnormalities are characterized by defects in the production of proinflammatory cytokines in response to lipopolysaccharide (LPS) stimulation, hypogammaglobulinemia, specific antibody deficiency, and natural killer cell dysfunction. Hematopoietic stem cell transplantation for X-EDA-ID has been employed as a curative treatment [6–10], but has sometimes resulted in engraftment failure.

NEMO colitis, which is inflammatory colitis associated with mutated NEMO protein [11], is found in one fifth of all X-EDA-ID patients [12] and is usually reported as inflammatory bowel disease (IBD), atypical colitis, or Behcet's disease [6, 11, 13]. The onset of inflammatory colitis occurs early in childhood and often causes failure to thrive [2, 5–7, 9, 11–13]. The age of onset of colitis in X-EDA-ID is earlier than that of Crohn's disease, ulcerative colitis, or chronic granulomatous disease [14]. Histological examination reveals active colitis with abundant neutrophilic infiltration, and the colitis usually improves with corticosteroids but not with antimicrobial agents [6, 11]. Susceptibility to colitis remains after hematopoietic stem cell transplantation [6, 9].

Recently, Nenci et al. demonstrated that mice lacking NEMO in intestinal epithelial cells developed spontaneous severe colitis [15]. However, an additional lack of tumor necrosis factor (TNF) receptor-1 in these mice inhibited intestinal inflammation. These interesting findings suggest that TNFα plays a role in the progression of NEMO colitis and that TNF blockade therapy would be a promising treatment.

We describe here an X-EDA-ID boy suffering from severe intractable colitis who improved dramatically following treatment with a chimeric anti-TNFα monoclonal antibody, infliximab. Infliximab administration reduced all symptoms relating to inflammatory colitis, not only frequent diarrhea and severe abdominal pain, but also inflammatory findings by colonoscopy. These effects have lasted for more than 2 years with regular administrations of infliximab.

Methods

Cell Preparation and Culture

Peripheral blood mononuclear cells (PBMCs) were isolated from peripheral blood from our X-EDA-ID patient and his mother using Ficoll-Paque gradient centrifugation. PBMCs were suspended in RPMI 1640 medium (Sigma-Aldrich, USA) and non-adherent cells were used to obtain stimulated T cells. Adherent cells were cultured for 10 days with 500 U/mL granulocyte-macrophage colony-stimulating factor (GM-CSF) (Peprotech, USA) to induce monocyte proliferation. T cells were stimulated for 48 h with 1-μg/mL phytohemaggulutinin (PHA) (Seikagaku Kogyo, Japan) and then for 8 days with 10-U/mL recombinant human interleukin (IL)-2 (Genzyme Techne, USA).

Cytokine Production Assay

PBMCs from our patient and healthy volunteers were incubated with LPS (1 μg/mL) (Sigma-Aldrich) at a concentration of 1×10^6 cells/mL at 37°C for 24 h. The concentration of TNFα in supernatant was measured using human BD OptEIA enzyme-linked immunosorbent assay kits (Becton-Dickinson, USA).

Mutation Analysis and Reversion Analysis

Genomic DNA from our patient and his mother was extracted from PBMCs, stimulated T cells, and stimulated monocytes using Puregene DNA purification kit (Gentra/Qiagen, USA); total RNA was extracted using TRIzol, according to the manufacturer's instructions (Invitrogen, USA). Complementary DNA (cDNA) was synthesized from total RNA with TaKaRa RNA PCR™ Kit (AMV) (Takara, Japan). Polymerase chain reaction (PCR) of genomic DNA and cDNA was performed using TaKaRa LA Taq (TaKaRa) with primers to amplify between exon 2 and exon 4 in the *IKBKG* gene. PCR primers were as follows: c1F, 5′-GCGCTCCTGAGACCCTCCAG-3′; c2R, 5′-GAGGAGAAGGAGTTCCTCAT-3′; G3F, 5′-CCCAGCTCCCCTCCACTGTC-3′; G4R, 5′-AACCCTG GAAGGGGTCTCCGGAG-3′. Genomic DNA was denatured at 94°C for 3 min, followed by 35 cycles of denaturation at 94°C for 30 s, annealing at 64°C for 30 s, and elongation at 68°C for 2 min 30 s, and a final extension for 7 min at 72°C using G3F and G4R primers. cDNA was denatured at 94°C for 1 min, followed by 35 cycles of denaturation at 94°C for 30 s, annealing and elongation at 68°C for 1 min, and a final extension for 5 min at 68°C using c1F and c2R primers. After gel electrophoresis and visualization, targeted bands were extracted and sequenced using ABI Big-Dye Terminator (Applied Biosystems, USA).

To analyze the reversion of mutation, we used our X-EDA-ID patient's PBMCs and stimulated cells. Mononuclear cells sorted with FACSVANTAGE (Becton-Dickinson) were used only at analysis after 12 months of infliximab treatment. PCR products were subcloned using a TOPO

TA cloning kit (Invitrogen) and sequenced as described above.

Reporter Assay for Detecting a Mutant NEMO Function: NEMO-NF-κB Luciferase Reporter Assay

NEMO cDNAs from a healthy volunteer and our patient were subcloned into the p3xFLAG-CMV14 vector (Sigma), respectively. NEMO null rat fibroblast cells (kindly provided by Dr. S. Yamaoka) were plated at a density of 3×10^4 cells/well in a 24-well culture dish and were transfected with 200 ng of plasmid, containing 40 ng of NF-κB reporter plasmid (pNF-κB-Luc; BD Biosciences Clontech, USA), 2 ng of a *NEMO* mutant expression construct, 148 ng internal control for normalization of transfection efficiency (pRL-TK; Toyo Ink, Japan), and the corresponding mock vector, using the FuGENE® HD Transfection Reagent (TOYO-B-Net, Japan) according to the manufacturer's protocol. At 12 h after transfection, the cells were stimulated with 15 ng/mL LPS for 4 h and the NF-κB activity was measured using the PicaGene® Dual SeaPansy assay kit (TOYO-B-NET) according to the manufacturer's protocol. Experiments were performed in triplicate and firefly luciferase activity was normalized to Renilla luciferase activity.

Vβ and Vα Analysis of T Cells

T cell receptor (TCR) β and α chain variable region (Vβ and Vα) repertoires were analyzed by a reverse transcription polymerase chain reaction (RT-PCR) method as described [16]. Briefly, each Vβ fragment (from Vβ1 to Vβ20) or Vα fragment (from Vα1 to Vα18, Vα21, and Vα24) was prepared from a series of HBVT/HBVP or HAVT/HAVP plasmids originating from thymus or peripheral T cells [17] and was dotted on filters. PCR products obtained from the patient by RT-PCR were labeled by α-^{32}P-dCTP and hybridized to the filters. Using densitometry, a semiquantitative assessment of V gene usage was made from the amounts of hybridized products.

Flow Cytometry

Peripheral blood samples were analyzed by three-color flow cytometry. Cells were stained with monoclonal antibodies to the following cell surface markers: CD3, CD4, CD8, CD19 (Becton-Dickinson), and CD14 (eBioscience, USA). Flow cytometry analysis of intracellular NEMO protein was performed as described previously [18]. Flow cytometric data from the stained cells were collected by FACScalibur and analyzed with CellQuest software (Becton-Dickinson).

Intracellular Cytokine Staining

Whole blood samples from our X-EDA-ID patient and healthy donors were stimulated with 1-μg/mL ionomycin (Sigma-Aldrich) and 25-ng/mL phorbol 12-myristate 13-acetate (PMA) (Sigma-Aldrich) in the presence of 10-μg/mL brefeldin A (Sigma-Aldrich) for 4 h. Cultured cells were stained with monoclonal antibodies against CD4 and CD8 for 30 min at room temperature. Stained cells were fixed and permeabilized with BD Lysing solution (Becton-Dickinson) and incubated with anti-TNFα monoclonal antibody or IgG1 isotypic control (Becton-Dickinson). Cells were analyzed by flow cytometry as described above. Analysis of intracellular TNFα in CD14+ cells was performed after stimulation with LPS (1 μg/mL) at 37°C for 4 h.

Endoscopy and Immunohistochemical Staining

Endoscopy was performed with the consent of legal guardians. Colon biopsies were obtained at regions of visual abnormalities. Formalin-fixed paraffin-embedded tissues blocks were cut into 2-μm sections and stained with hematoxylin and eosin. Subsequently, immunohistochemical analysis using the following primary antibodies with optimized experimental protocols was performed: CD3ε (DAKO, Denmark, rabbit, polyclonal, diluted 1:100, incubated for 24 h at 4°C after microwave heat-induced antigen retrieval for 40 min in pH 6.0 citrate buffer), CD79a (DAKO, mouse, monoclonal, 1:100, microwave for 40 min, pH 6.0), CD68 (DAKO, mouse, monoclonal, 1:50, proteinase K (DAKO) for 10 min at room temperature), CD4 (Novocastra, USA, 1:100, microwave for 40 min, pH 9.0 (NICHIREI BIOSCIENCES, Japan)), CD8 (DAKO, mouse, monoclonal, 1:100, microwave for 40 min, pH 9.0), and TNFα (Santa Cruz Biotechnology, USA, goat, polyclonal, 1:200, microwave for 40 min, pH 6.0). An Envision-HRP Detection kit (DAKO) was used for visualization, except for anti-TNFα, which was visualized using donkey biotin conjugated anti-goat secondary antibody (Jackson ImmunoResearch Laboratories, USA) and LASB2-System/HRP kit (DAKO).

Infliximab Treatment

Infliximab treatment for our X-EDA-ID patient was approved by the medical ethics committee of the University of Miyazaki. We obtained written consent concerning treatment from both the patient and his guardian. Before initiating infliximab, we confirmed that he had no severe infection including tuberculosis according to laboratory data, mycobacterium culture test, skin tuberculin test, and chest computed tomography. Cardiac dysfunction was excluded by echocardiography and electrocardiogram.